electronics

Article

A New Geomagnetic Vector Navigation Method Based on a Two-Stage Neural Network

Zhuo Chen, Zhongyan Liu *, Qi Zhang, Dixiang Chen, Mengchun Pan and Yujing Xu

College of Artificial Intelligence, National University of Defense Technology, Changsha 410073, China; chenzhuo@nudt.edu.cn (Z.C.); 13873191345@163.com (Q.Z.); chendixiang@163.com (D.C.); pmc1958@163.com (M.P.); xuyujing@nudt.edu.cn (Y.X.)

* Correspondence: liuzhongyan@nudt.edu.cn

Abstract: The traditional geomagnetic matching navigation method is based on the correlation criteria operations between measurement sequences and a geomagnetic map. However, when the gradient of the geomagnetic field is small, there are multiple similar data in the geomagnetic database to the measurement value, which means the correlation-based matching method fails. Based on the idea of pattern recognition, this paper constructs a two-stage neural network by cascading a probabilistic neural network and a non-fully connected neural network to, respectively, classify geomagnetic vectors and their feature information in two steps: "coarse screening" and "fine screening". The effectiveness and accuracy of the geomagnetic vector navigation algorithm based on the two-stage neural network are verified through simulation and experiments. In simulation, it is verified that when the geomagnetic average gradient is 5 nT/km, the traditional geomagnetic matching method fails, while the positioning accuracy based on the proposed method is 40.17 m, and the matching success rate also reaches 98.13%. Further, in flight experiments, under an average gradient of 11 nT/km, the positioning error based on the proposed method is 39.01 m, and the matching success rate also reaches 99.42%.

Keywords: geomagnetic vector field; geomagnetic navigation; two-stage neural network; pattern recognition

Citation: Chen, Z.; Liu, Z.; Zhang, Q.; Chen, D.; Pan, M.; Xu, Y. A New Geomagnetic Vector Navigation Method Based on a Two-Stage Neural Network. *Electronics* **2023**, *12*, 1975. https://doi.org/10.3390/electronics12091975

Academic Editor: Arturo de la Escalera Hueso

Received: 28 March 2023
Revised: 15 April 2023
Accepted: 20 April 2023
Published: 24 April 2023

1. Introduction

As the inherent physical field of the Earth, the geomagnetic field has a one-to-one correspondence with geographical location. More than 98% of the Earth can use geomagnetic information for navigation [1,2]. Geomagnetic navigation, as a passive, autonomous, and highly covert navigation method, is a reliable and stable alternative to satellite navigation under denied conditions [3–5]. The geomagnetic vector field has more information than the geomagnetic scalar field, so it can improve the accuracy and anti-interference ability for navigation [6–8]. However, as the intensity or gradient of the geomagnetic field increases with height, it will decay exponentially [9,10]. Therefore, when utilizing geomagnetic information for navigation on aircraft and other aviation platforms, it is inevitable that the problem of navigation under small-gradient geomagnetic fields will arise, which poses new challenges to geomagnetic vector navigation.

At present, whether utilizing geomagnetic scalar information or geomagnetic vector elements for navigation, all methods are based on relevant principles to match geomagnetic measurement sequences with geomagnetic databases. The iterative closest contour point (ICCP) algorithm [11–15] and the magnetic contour matching (MAGCOM) algorithm [15–20] are two widely studied and applied geomagnetic navigation algorithms based on correlation matching. Correlation criteria mainly include the product correlation algorithm (PROD), mean absolute difference (MAD), mean square difference (MSD), and normalized product correlation algorithm (NPROD). However, there is a common and insurmountable problem based on correlation matching algorithms: When the geomagnetic gradient is relatively small, the value of the data in the geomagnetic database near the track sampling point is very similar. The results calculated by the above correlation criteria often fail to distinguish the geomagnetic values corresponding to the real path from these similar data, resulting in mismatching problems [21,22].

Geomagnetic navigation can be considered as a special case of comparative navigation. With the development of machine learning technology, neural networks have become a popular and effective tool to solve nonlinear classification problems, being applied in comparative navigation. Andrzej S., from Maritime University, computed a ship's position plot by using artificial neural networks, which changes the image given at its input (image segment) into the index of one of its neurons [23]. The return number obtained corresponds to the neuron that is closest to the input image according to the selected metric. These steps are similar to the geomagnetic matching process. Mohammed A. from King Saud University compared the performance of four kinds of fuzzy logic in the navigation and control of a mobile robot in an unstructured environment, including manually constructed fuzzy logic (M-Fuzzy), fuzzy logic with genetic algorithm (GA-Fuzzy), fuzzy logic with neural network (Neuro-Fuzzy), and fuzzy logic with PSO (PSO-Fuzzy) [24]. The performances of both PSO-Fuzzy and Neuro-Fuzzy were found to be better than the other methods in terms of navigation distance travelled, proving the development prospects of navigation based on neural network algorithms. Andrzej S. proposed a method for the fast processing of 3D multibeam sonar data to make the depth area comparable with areas from bathymetric electronic navigational charts as source maps during comparative navigation. In this method, an artificial neural network (ANN) is trained to realize depth area images registered in semi-real time [25]. Given the applicability and effectiveness of a neural network in the comparative navigation, this technology has also been preliminarily developed and applied in geomagnetic navigation, which shows potential for application in small-gradient geomagnetic fields. Some improvements start with improving the accuracy of the geomagnetic database: Kim D. from Korea Advanced Institute of Science and Technology utilized convolutional neural networks (CNNs) to expand and optimize geomagnetic database data and used relevant matching algorithms to achieve geomagnetic navigation [26]; Qiong W. from Northwestern Polytechnical University reconstructed the geomagnetic database of the matching region using a BP neural network and implemented geomagnetic navigation based on a triangular matching algorithm [27]. Although the above two methods optimized the geomagnetic database through different neural networks, they are still based on the principle of correlation to find the closest points to the magnetic field of the measurement sequence. Therefore, they did not significantly improve the application in small-gradient geomagnetic field environments. Zhou J. from Northwestern Polytechnical University performed pattern recognition and matching on geomagnetic total measurement sequences based on probabilistic neural networks (PNNs), enabling geomagnetic navigation under geomagnetic scalar field with a small gradient. However, they did not further analyze whether the identification result is the best path, and matching based on one-dimensional total information results in insufficient robustness and practicality of the algorithm [28].

To solve this problem, this paper constructs a two-stage neural network model by cascading PNN networks and non-fully connected neural networks, and it proposes a geomagnetic vector navigation method based on two-stage neural networks. The matching area and the category to be matched are delimited according to the INS reference path, and probabilistic neural networks are utilized as the first stage classifier model to conduct large-scale rapid screening. We set the probability value range of the PNN output and output the corresponding mode class. Then, a non-fully connected neural network is utilized as the second-stage classifier, and the statistical features of the geomagnetic vector corresponding to the first-stage output pattern class are selected as the network input. The accurate screening of the second stage ultimately establishes the best matching path and achieves high-precision navigation of the areas with poor geomagnetic information.

2. Geomagnetic Vector Pattern Recognition Based on PNN

Due to the nonlinear mapping relationship between geomagnetic vectors and geographical coordinates, classification methods based on mathematical theory can easily mismatch or fail completely when geomagnetic features in the navigation area of an aviation platform are not significant. As a PNN mainly utilized in the field of pattern recognition, it introduces Bayesian classification decisions into the neural network based on probability density estimation methods and sets the network structure according to Bayesian discriminant functions, thereby ensuring high accuracy in the nonlinear learning algorithms and minimizing error rates or losses. Therefore, this section constructs a PNN network structure for geomagnetic vector pattern recognition navigation.

2.1. Geomagnetic Vector Pattern Recognition Navigation Principles

Pattern recognition divides samples into certain categories based on their characteristics. For geomagnetic vector matching navigation, the essence of the problem is to establish some samples to be identified and use known magnetic vector information for classification and recognition. Therefore, the description of the geomagnetic vector pattern recognition matching navigation method is as follows: in the matching area, take the real track measurement sequence as the target, construct the track to be matched as the pattern class to be matched, train and implement pattern matching classification based on neural networks according to certain criteria, and the pattern class with the highest similarity to the target class is the final output matching result.

Specifically, the principle of geomagnetic pattern recognition navigation is shown in Figure 1. From time t_{h-n+1} to t_h, the carrier has a segment of track L in the matching area. There are n sampling points on the track L, and a series of geomagnetic vector measurement sequences $f\left(X_{t_h}, X_{t_{h-1}}, \cdots, X_{t_{h-n+1}}\right)$ are collected. Each X_t includes the geomagnetic scalar Bt, the geomagnetic north component Bn, the geomagnetic east component Be, and the geomagnetic vertical component Bd. With the last sampling point C of the track L as the center point and the inertial navigation error range as the boundary, a grid area is expanded, with a and b being the number of grids in the transverse and longitudinal directions, respectively. Therefore, $m = (2a+1)(2b+1)$ grid points are constructed in the matching region. Record the grid points as (1, 2, . . . m) from top to bottom and from left to right. Using m grid points as the last point, m similar tracks are generated according to the sampling interval of the inertial navigation path. Each track also has n sampling points, which contains the corresponding geomagnetic vector data. Taking the wth track as an example, it is the track generated from the wth grid point, corresponding to geomagnetic vector measurement sequence $f\left(X_{wn}, X_{w(n-1)}, \cdots, X_{w1}\right)$, which is defined as the wth pattern class. According to the idea of pattern recognition, m tracks are corresponding m pattern classes to be matched. The process of finding a pattern grid is compared to the geomagnetic vector measurement sequence of the real track Lr with the geomagnetic vector information on m patterns' $f\left(X_{wn}, X_{w(n-1)}, \cdots, X_{w1}\right)$, and the best-matched pattern is selected as the optimized track as an output result.

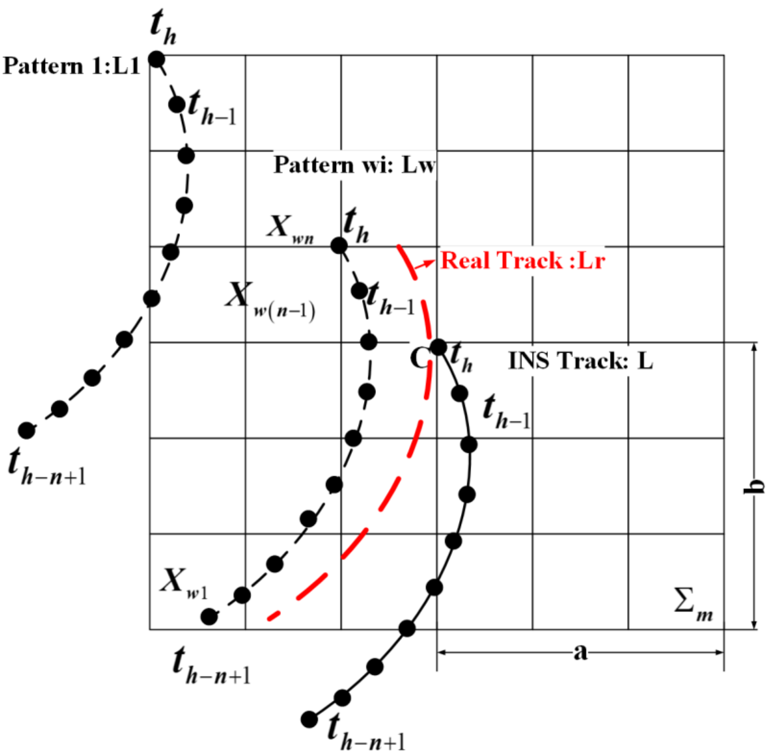

Figure 1. Principles of geomagnetic pattern recognition navigation.

Set the INS longitude and latitude coordinate as (λ, φ). The calculation formula for the sampling point interval of the wth mode class is as follows:

$$\Delta\lambda_{w_i} = |\lambda(t_h) - \lambda(t_{h-i+1})|, i = 1, 2, \cdots, n \tag{1}$$

$$\Delta\varphi_{w_i} = |\varphi(t_h) - \varphi(t_{h-i+1})|, i = 1, 2, \cdots, n \tag{2}$$

2.2. Geomagnetic Vector Pattern Recognition Based on PNN

2.2.1. PNN Models

The geomagnetic vector pattern recognition navigation method based on PNN consists of steps, such as magnetic map grid division, pattern class generation, PNN network construction, and pattern recognition matching. The geomagnetic vector test sample of the reference path is used as the network input, and Bayesian maximum likelihood estimation is performed by calculating the Euclidean distance and corresponding Gaussian functions between the input sample and all mode classes in the test set. The neurons of the Gaussian function in the mode layer are activated, and an initial probability matrix is established. The sum of probabilities of each sample belonging to each type is obtained at the summation layer. The mode class with the highest probability is selected, and its number is used as the output of the network. Find the current optimal path through the corresponding output mode class number.

The algorithm flow is described as follows: The search area is generated based on the endpoint of the test path and is divided into m grid points as the endpoint of m pattern classes, with each pattern class having a dimension of n. X_{ik} is the Kth training sample belonging to pattern class w. Send it into PNN, calculate the Euclidean distance and Gaussian function between samples, and obtain an initial probability matrix $p_{w_i}(X_{ik})$ with dimension $\mathbb{R}^{m \times n}$. The Gaussian function formula [29] is as follows:

$$g_{w_i}(X, \sigma) = \frac{1}{n_i} \sum_{k=1}^{ni} \exp^{-\frac{\|X - X_{ik}\|^2}{\sigma^2}}, i \in (1, 2, \cdots, m) \tag{3}$$

When the neurons of the Gaussian function are activated, the initial probability matrices $p_{w_i}(X_{ik})$ with a quantity of J are obtained. Then, sum to obtain the initial probability and matrix S of the sample under various smoothing factors, with a dimension of $\mathbb{R}^{m \times n \times J}$. Calculate the probability:

$$prob_{ij} = \frac{S_{ij}}{\sum_{i=1}^{M} S_{in}} (j = 1, 2, \cdots, J) \quad (4)$$

Select the pattern class with the highest probability value as the correct pattern class $r_j = \max(prob_{ij})$ for classification. The PNN network model determined based on the above steps is shown in Figure 2.

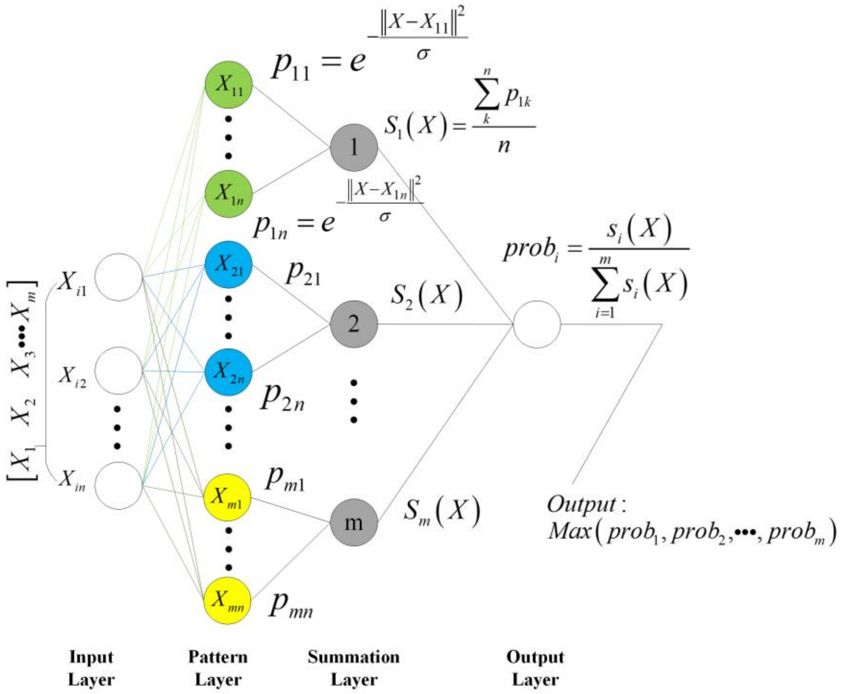

Figure 2. PNN model.

The network consists of an input layer, a sample layer, a summation layer, and a competition (output) layer. The number of neurons in the input layer is the characteristic vector, which is the dimension of each pattern class sample. In the input layer, the network calculates the Euclidean distance between the input vector and all training sample vectors. The number of neurons in the mode layer is the number of training samples. This layer is a nonlinear calculation layer, and the activation function is a Gaussian function. The Gaussian function is activated through the Euclidean distance between samples and set smoothing parameters to achieve initial probability calculation for input samples, and the output is transmitted to the summation layer. The number of neurons in the summation layer is the number of pattern categories. Its function is to sum the output of the pattern layer by class, equivalent to an adder. Finally, the probability that the sample belongs to each category is calculated at the competition level, and the category with the largest probability value is used as the unique output of the model.

There are m types of training samples, and if the dimensions of each type are n, the total number of samples is $T = m \times n$. Thus, the number of input layer nodes is n. T is the corresponding number of mode layer nodes, which is divided into m sets of nodes, corresponding to the number of m nodes in the summation layer. For the geomagnetic vector pattern recognition method, combined with Formulas (1) and (2), the longitude and latitude coordinates of the wth training sample (the wth track) at time t_{h-i+1} are:

$$\begin{array}{l} \lambda_w\left(t_{h-i+1}\right) = \lambda_w(t_h - i) - \Delta\lambda_{w_i}, \quad i = 1, 2, \cdots, n \\ \varphi_w\left(t_{h-i+1}\right) = \varphi_w(t_h - i) - \Delta\varphi_{w_i}, \quad i = 1, 2, \cdots, n \end{array} \tag{5}$$

The expression of the geomagnetic vector sampling sequence vector X_{ik} for this w mode is as follows:

$$\begin{cases} X_{ik} = [F_1(\lambda_w(t_{h-i+1}), \varphi_w(t_{h-i+1})), F_2(\lambda_w(t_{h-i+1}), \varphi_w(t_{h-i+1})), \cdots, F_4(\lambda_w(t_{h-i+1}), \varphi_w(t_{h-i+1}))] \\ \\ X_{ik} = \begin{bmatrix} F_1(\lambda_w(t_{h-n+1}), \varphi_w(t_{h-n+1})), F_2(\lambda_w(t_{h-n+1}), \varphi_w(t_{h-n+1})), \cdots, F_4(\lambda_w(t_{h-n+1}), \varphi_w(t_{h-n+1})) \\ \cdots \quad \cdots \quad \cdots \\ F_1(\lambda_w(t_h), \varphi_w(t_h)), \quad F_2(\lambda_w(t_h), \varphi_w(t_h)) \quad , \quad \cdots, \quad F_4(\lambda_w(t_h), \varphi_w(t_h)) \end{bmatrix} \end{cases} \tag{6}$$

where F_1 is the geomagnetic scalar value of the measurement sequence on the w mode track, F_2 is the geomagnetic north component measurement sequence, F_3 is the geomagnetic east component measurement sequence, and F_4 is the geomagnetic vertical component measurement sequence. All m pattern vectors are normalized to form a training matrix D.

$$D = \begin{bmatrix} X_{11} & X_{21} \cdots X_{1m} \\ & \cdots \\ X_{1i} & X_{2i} \cdots X_{km} \\ & \cdots \\ X_{1m} & X_{2m} \cdots X_{nm} \end{bmatrix} = \left[X_1 X_2 \cdots X_m\right] \tag{7}$$

The normalized training sample set is $X_i, i = 1, 2, \cdots, m$. Then, the training matrix D corresponding to the label matrix (pattern class matrix) is $Q = \left[12 \cdots m\right]$.

Calculate the Euclidean distance between the normalized sample to be classified and all training samples to form the Euclidean distance matrix E:

$$E = \begin{bmatrix} \sqrt{\sum\limits_{k=1}^{n} |Y_{1k} - X_{1k}|^2} & \sqrt{\sum\limits_{k=1}^{n} |Y_{1k} - X_{2k}|^2} \cdots \sqrt{\sum\limits_{k=1}^{n} |Y_{1k} - X_{mk}|^2} \\ \sqrt{\sum\limits_{k=1}^{n} |Y_{2k} - X_{1k}|^2} & \sqrt{\sum\limits_{k=1}^{n} |Y_{2k} - X_{2k}|^2} \cdots \sqrt{\sum\limits_{k=1}^{n} |Y_{2k} - X_{mk}|^2} \\ \cdots & \cdots \quad \cdots \quad \cdots \\ \sqrt{\sum\limits_{k=1}^{n} |Y_{lk} - X_{1k}|^2} & \sqrt{\sum\limits_{k=1}^{n} |Y_{lk} - X_{2k}|^2} \cdots \sqrt{\sum\limits_{k=1}^{n} |Y_{lk} - X_{mk}|^2} \end{bmatrix} = \begin{bmatrix} E_{11} & E_{12} & \cdots E_{1m} \\ E_{21} & E_{22} & \cdots E_{2m} \\ \cdots & \cdots & \cdots \quad \cdots \\ E_{l1} & E_{l2} & \cdots E_{lm} \end{bmatrix} \tag{8}$$

Normalized samples to be classified are $Y_u, u = 1, 2, \cdots, l$. E_{ui} represents the Euclidean distance between the uth training sample to be classified and the ith training sample.

Enter the smoothing factor σ. Activate the neurons of the Gaussian function in the mode layer to obtain the initial probability matrix:

$$P = \begin{bmatrix} e^{-\frac{E_{11}}{2\sigma^2}} & e^{-\frac{E_{12}}{2\sigma^2}} \cdots e^{-\frac{E_{1m}}{2\sigma^2}} \\ e^{-\frac{E_{21}}{2\sigma^2}} & e^{-\frac{E_{22}}{2\sigma^2}} \cdots e^{-\frac{E_{2m}}{2\sigma^2}} \\ \cdots & \cdots \quad \cdots \quad \cdots \\ e^{-\frac{E_{l1}}{2\sigma^2}} & e^{-\frac{E_{l2}}{2\sigma^2}} \cdots e^{-\frac{E_{lm}}{2\sigma^2}} \end{bmatrix} = \begin{bmatrix} P_{11} & P_{12} & \cdots P_{1m} \\ P_{21} & P_{22} & \cdots P_{2m} \\ \cdots & \cdots & \cdots \quad \cdots \\ P_{l1} & P_{l2} & \cdots P_{lm} \end{bmatrix} \tag{9}$$

The number of samples is T, which can be divided into m categories. The dimension of each type of sample is n, and the initial probability sum of each type of sample can be obtained at the summation layer of the network:

$$S = \begin{bmatrix} \sum_{k=1}^{n} P_{1k} & \sum_{k=\mathrm{n}+1}^{2n} P_{1k} \cdots & \sum_{k=T-\mathrm{n}+1}^{T} P_{1k} \\ \sum_{k=1}^{n} P_{2k} & \sum_{k=\mathrm{n}+1}^{2n} P_{2k} \cdots & \sum_{k=T-\mathrm{n}+1}^{T} P_{2k} \\ \cdots & \cdots \quad \cdots & \cdots \\ \sum_{k=1}^{n} P_{lk} & \sum_{k=\mathrm{n}+1}^{2n} P_{lk} \cdots & \sum_{k=T-\mathrm{n}+1}^{T} P_{lk} \end{bmatrix} = \begin{bmatrix} S_{11} & S_{12} & \cdots S_{1m} \\ S_{21} & S_{22} & \cdots S_{2m} \\ \cdots & \cdots & \cdots \quad \cdots \\ S_{l1} & S_{l2} & \cdots S_{lm} \end{bmatrix} \tag{10}$$

The probability that the uth sample belongs to the ith category can be calculated as:

$$prob_{ui} = \frac{S_{ui}}{\sum\limits_{i=1}^{m} S_{ui}} \tag{11}$$

Finally, the corresponding pattern class corresponding to the maximum probability is obtained as the network recognition matching result output:

$$output = Pattern[\max(prob_{ui})] \tag{12}$$

2.2.2. Pattern Recognition Algorithm Based on PNN

The geomagnetic vector pattern recognition algorithm based on PNN parameter optimization can be summarized into the following steps:

1. During the driving process in the matching area, the carrier outputs the INS reference track L, divides a grid area with m grid points based on the end point C of track L and the INS error range, and determines m mode classes;
2. Determine training samples and corresponding labels according to Equations (4)–(7), normalize sample data, and calculate the Euclidean distance matrix between samples;
3. Follow these steps to build a PNN:
   ① Input layer has m nodes. The number of nodes in the mode layer is equal to the number of training samples T. Each node has a deviation. The number of nodes in the summation layer is the same as the number of pattern classes m. The output layer has only one node, which makes Bayesian decisions;
   ② Calculate the geomagnetic vector roughness of the matching region as the network parameters σ, and construct a PNN network by substituting it into the activation function of Equation (8). The calculation formula for geomagnetic roughness [30] is as follows:

$$\begin{cases} \sigma_x = \sqrt{\frac{1}{a(b-1)} \sum\limits_{i=1}^{a} \sum\limits_{j=1}^{b-1} \left(f(i,j) - \overline{f} \right) \left(f(i,j+1) - \overline{f} \right)} \\ \sigma_y = \sqrt{\frac{1}{(a-1)b} \sum\limits_{i=1}^{a-1} \sum\limits_{j=1}^{b} \left(f(i,j) - \overline{f} \right) \left(f(i+1,j) - \overline{f} \right)} \end{cases} \tag{13}$$
$$\sigma = \frac{\sigma_x + \sigma_y}{2}$$

where ρ_x and ρ_y represent the transverse and longitudinal roughness of the two-dimensional magnetic map, respectively. $f(i,j)$ is the value of the two geomagnetic components at the coordinate point (i, j), and $\overline{f}$ is the average value of each component in the search area on each pattern class.

4. According to Equations (8) and (9), activate the Gaussian function of the mode layer, calculate the Gauss matrix corresponding to the Euclidean distance matrix of the sample, further obtain the probability and matrix of the sample belonging to various types, and determine the geomagnetic vector pattern recognition navigation PNN model;
5. Input normalized samples $Y_u, u = 1, 2, \cdots, l$ to be identified. Perform Bayesian maximum likelihood estimation and classification according to Formulas (7) to (11), and identify them as belonging to the category with the highest probability among the m pattern classes: $Pattern[\max(prob_{ui})]$. The track corresponding to this pattern class is determined as the optimal matching track.

2.3. Algorithm Performance and Shortage

Firstly, the effectiveness of the pattern recognition algorithm based on PNN is verified in the simulation of a small-gradient geomagnetic field. The simulation parameter settings are shown in Table 1.

Table 1. Simulation preset parameters.

Parameters	Value
geomagnetic field size	20 km × 20 km
grid size	100 m × 100 m
geomagnetic gradient	5~11 nT/km
sample points number	10
measurement error	N(0,20)nT
INS track error	(1600 m, 1600 m)

The result of the pattern recognition PNN algorithm is shown in Figure 3 and Table 2. The success rate is defined as the ratio of the number of points located within a grid to the total number of track points.

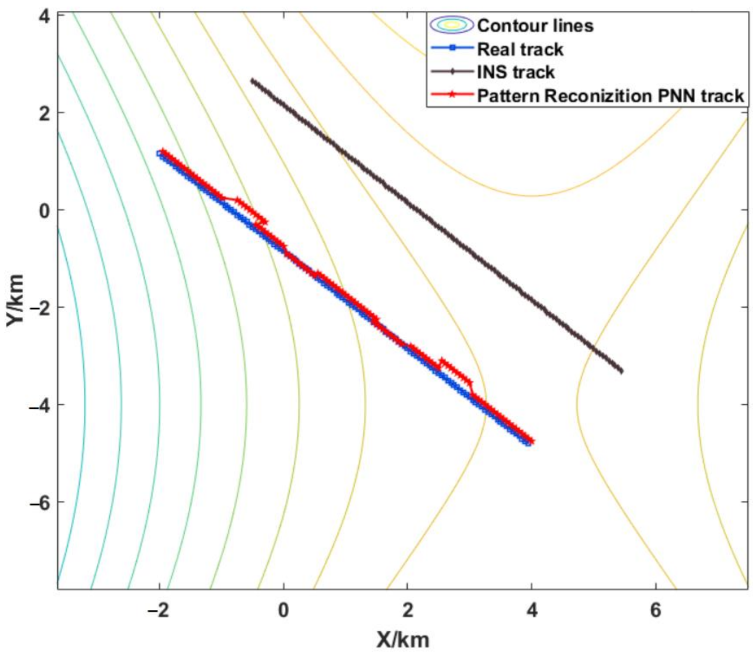

Figure 3. Positioning result of pattern recognition PNN.

Table 2. Positioning result of pattern recognition navigation algorithm based on PNN.

Evaluating Indicator	Pattern Recognition PNN
average position error/m	101.42
standard deviation/m	68.95
success rate	83%

From the results shown in Figure 3 and Table 2, the geomagnetic vector pattern recognition algorithm based on PNN can achieve geomagnetic vector navigation well, but the average positioning error exceeds one grid, and the success rate does not reach 90%. The main reason is that, according to the PNN model, the optimal output solution of pattern matching is the corresponding probability maximum pattern class. However, due to the fact that the network pattern samples contain only geomagnetic two-component and total magnetic field information, the matching probability distinction on similar pattern classes is not obvious. Take a segment pattern recognition PNN navigation probability calculation result; the matching path is shown in Figure 4. The corresponding probability value and matching error of the pattern number are shown in Table 3.

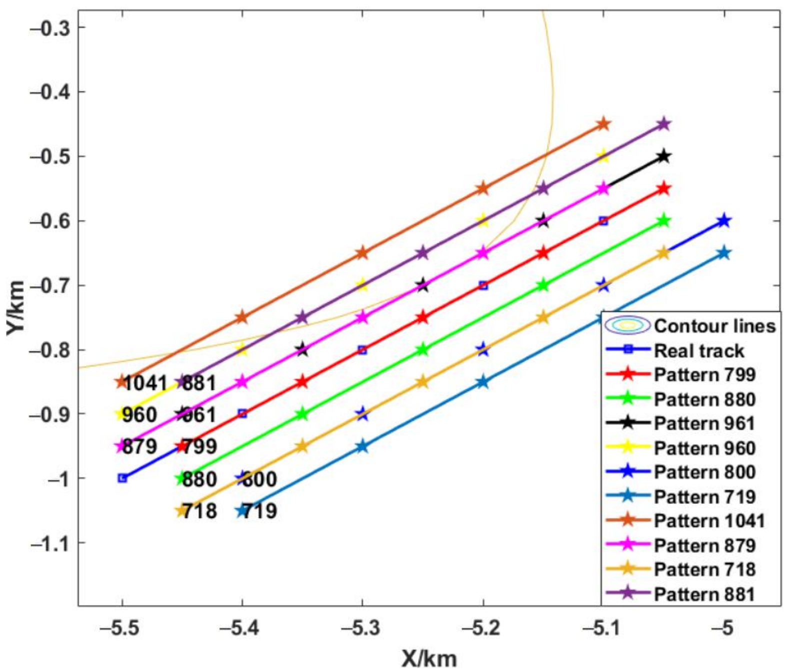

Figure 4. Probabilistic top 10 patterns of pattern recognition navigation based on PNN.

Table 3. Comparison of matching results of three algorithms.

Pattern Number	Probability Value	Position Error/m
880	0.999997	70.77
799	0.999981	50.01
961	0.999980	111.82
960	0.999959	100.04
800	0.999958	100.75
719	0.999955	111.81
1041	0.999954	150.02
879	0.999930	75.00
718	0.999926	100.04
881	0.999920	158.13

According to the results in Figure 4 and Table 3, the closest track to the real path should be the red track. The corresponding pattern class number is "799", but the corresponding pattern class for the maximum PNN output probability is the "880" pattern class corresponding to the green path with a probability value of 0.999997. This indicates that the maximum probability pattern class obtained by network calculation cannot guarantee that it is necessarily the best matching track, but it may be the second best or even the worst matching track.

3. Geomagnetic Vector Navigation Based on Two-Stage Neural Network

To solve the problem of the pattern recognition navigation algorithm based on PNN, a new geomagnetic vector navigation method based on a two-stage neural network is proposed. The PNN is set as the first stage in the two-stage model, and its output is not only the pattern class corresponding to the highest probability but also those pattern classes corresponding to the probabilities at 98%. A non-fully connected network is designed as the second stage of the model. The statistical characteristics of the geomagnetic vector of output pattern class tracks are the new inputs to the second stage to finish the accurate screening of the optimal track.

3.1. Two-Stage Neural Network Model Design

To implement the classification function using a non-fully connected neural network, it is necessary to first determine the learning training samples and obtain a training model suitable for geomagnetic vector data classification. Secondly, on the basis of completing the training, the output of the PNN classifier is changed from the maximum unique probability value to a preset probability range value (98%), and the statistical feature set of the geomagnetic vector elements of the corresponding pattern class track are selected as the inputs of the non-fully connected network to perform a two-stage accurate screening to obtain the optimal classification result.

According to the above design, a basic classification algorithm flowchart of the two-stage neural network is shown in Figure 5.

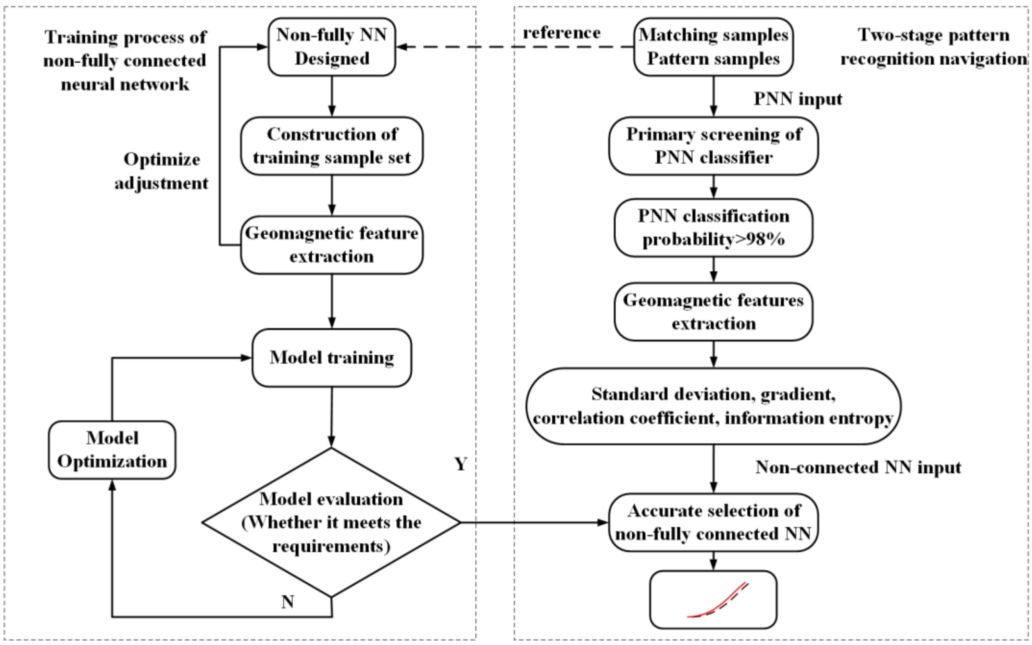

Figure 5. Two-stage pattern recognition navigation algorithm flowchart.

The first-stage model of the two-stage network was clarified, so the key point of constructing the network model is then to determine the structure of the second-stage non-fully connected network model. Theoretically, the number of neural network layers is positively correlated with accuracy, but as the number of layers increases, the operation time will increase by different multiples or even exponentially depending on different network models.

The commonly used characteristic parameters of geomagnetic fields include seven items, such as standard deviation, information entropy, gradient information, skewness/kurtosis coefficient, and roughness, which reflect the characteristics of regional magnetic fields from different or approximate aspects. However, for a neural network and geomagnetic pattern recognition, using more parameters does not translate to a better classification effect. In order to obtain a better classification effect, the feature parameters generally need to be representative rather than high-dimensional. For geomagnetic navigation, some irrelevant and redundant features do not have good classification capabilities. According to the literature [31], the four characteristic parameters of geomagnetic standard deviation, information entropy, average gradient, and minimum gradient within the region during vector matching have better classification capabilities in neural networks.

For geomagnetic navigation on the carriers, it requires faster calculation and output speed for the whole network. Due to the fact that the non-fully connected neural network in the two-stage network only needs to establish a limited number of model representations of feature parameters to pattern tracks, it does not require overly complex network structures. Therefore, in the non-fully connected neural network, a four-layer network model structure of "input-hide-hide-output" with two hidden layers is adopted. Considering the three sets of four characteristic parameters composed of geomagnetic vector elements, the input layer nodes corresponding to the three networks are, respectively, 4, and the hidden layer nodes are set to 8 based on experience. The structure for the three vector and one scalar elements in the non-fully connected model is $4 \times 8 \times 8 \times 1 \times 1$.

The structure of the two-stage network model based on PNN and non-fully connected neural networks is shown in Figure 6.

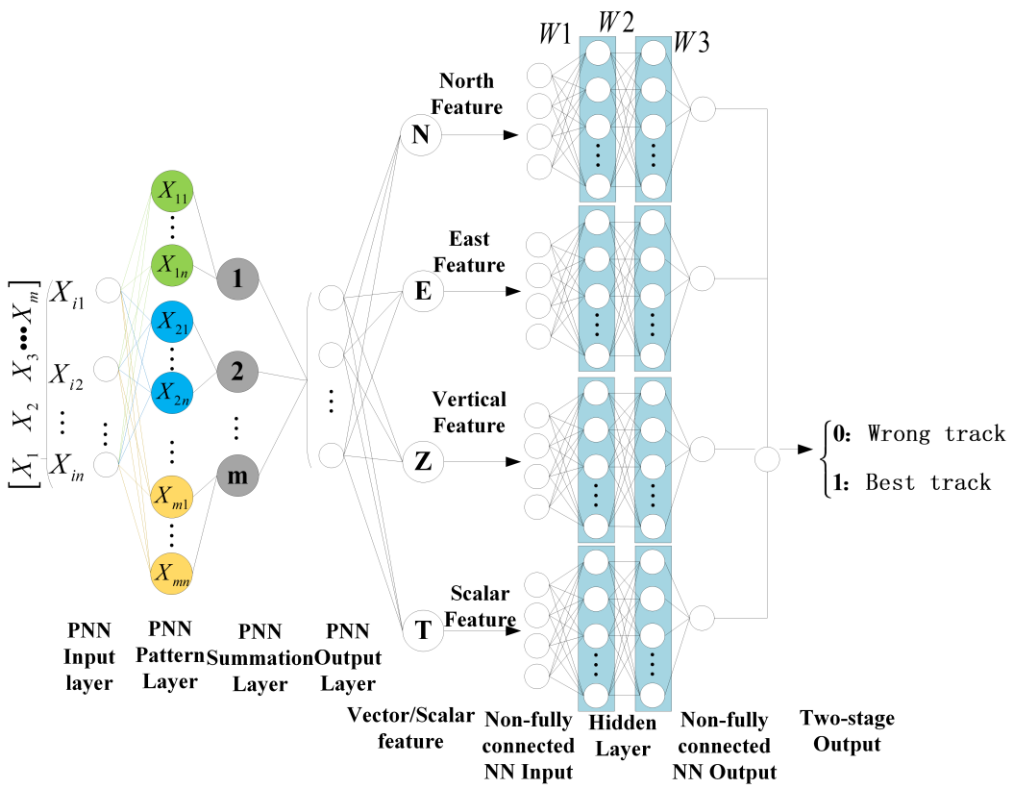

Figure 6. Two-stage neural network model.

In Figure 6, the PNN input layer is a geomagnetic vector and scalar data for each pattern class sequence and measured sequence in the navigation region. The PNN output layer is pattern class tracks with calculated pattern matching probability greater than 98%. After calculating the corresponding geomagnetic vector and scalar characteristics of the track, it is utilized as four sets of network input matrices for the non-fully connected NN input layer, with the size of each set of input characteristic matrices being $\mathbb{R}^{4*100}$. For the outputs of the non-fully connected NN, the calculation results of its respective component network are obtained. Finally, at the two-stage output layer, four sets of results are synthesized for final label classification to obtain the optimal matching track.

3.2. Activation Function and Evaluation Index

The activation function of a network is the most important parameter for solving nonlinear problems. A reasonable activation function can make the network more powerful and accurate in expressing the model.

As shown in Figure 6, the output of the two-stage NN is a problem in binary classification. For binary classification problems, the most commonly used output layer is the sigmoid function. The mathematical expressions for the sigmoid function are shown in Figure 7.

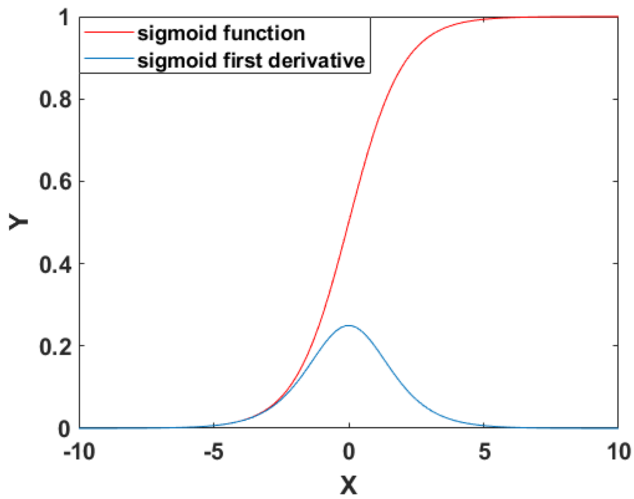

Figure 7. Sigmoid function.

As the activation function of the output layer, the output value of the sigmoid represents the sample label probability. The geomagnetic matching binary classification problem is the probability of incorrect matching and accurate matching. Since the sigmoid output is a continuous value between 0 and 1, it is necessary to set a threshold value for binary classification. Generally, it is bounded by 0.5. If it is greater than 0.5, it is labeled as 1, and if it is greater than 0.5, it is labeled as 0. However, in geomagnetic navigation, due to the high requirements for positioning probability, the label division threshold should be closer to 1, rather than the traditional 0.5. In this article, the threshold is set to 0.85.

For the entire network, the weights W and bias B of the neural network are solved via a gradient descent update. In the reverse transfer process, the derivative of the sigmoid function is less than 1, especially when it approaches the saturation region, and the derivative approaches 0, leading to the disappearance of the gradient, which leads to an inability to converge or extremely slow convergence in the network. Therefore, the hidden layer activation function selects the ReLU function to solve the gradient disappearance problem existing in the sigmoid function, which is shown in Figure 8.

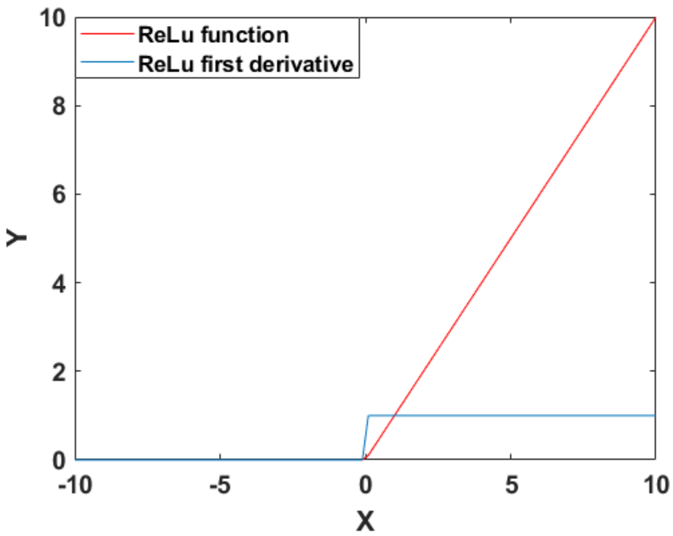

Figure 8. ReLU function.

Through the two types of activation functions in the output layer and the hidden layer, both the accuracy and efficiency of network classification are ensured, and the gradient disappearance problem is avoided, which can better adapt to the geomagnetic navigation binary classification problem.

It is known that the two-stage neural-network-based geomagnetic navigation method is essentially a binary classification problem. There are four classification judgment results for the binary classification problem, which are represented by True Positive (TP), False Positive (FP), False Negative (FN), and True Negative (TN), as shown in Table 4.

Table 4. Neural network binary classification judgment results.

Estimated Value / True Value	1	0
1	TP	FN
0	FP	TN

Based on the data of the four judgment results, the accuracy rate P, detection rate P_d, and false alarm rate P_f of the binary classification can be calculated, thereby determining the accuracy of the neural network classification results. The calculation formula for the above three indicators is as follows:

$$\begin{cases} P = \frac{TP+TN}{TP+FN+FP+FN} \\ P_d = \frac{TP}{TP+FN} \\ P_f = \frac{FP}{FP+TN} \end{cases} \tag{14}$$

To ensure the accuracy of the two-stage neural network pattern recognition, it is necessary to ensure that p is as high as possible while keeping P_f as low as possible.

3.3. Feature Parameter Extraction

As previously mentioned, four representative types of geomagnetic characteristic parameters can be calculated based on the geomagnetic vector and scalar elements on the track: the standard deviation δ (G1~G4), gradient S (G5~G8), correlation coefficient ρ (G9~G12), and information entropy (G13~G16). As shown in Figure 1, the sample track dimension in the grid navigation area is n, and a and b are the number of horizontal and vertical grid points in the area where the sample track is located. The coordinates of each point are (λ, φ). Since the calculation formulas for the corresponding characteristic parameters of each geomagnetic element at point (λ, φ) are the same, the only difference is that the input quantities utilized to calculate the characteristic parameters are the geomagnetic scalar or vector values. Therefore, a unified expression and calculation formula are given, and the four variables can be calculated separately. The geomagnetic vector and scalar elements at point (λ, φ) are uniformly expressed as a $f(\lambda, \varphi)$.

The standard deviation of the geomagnetic field represents the difference between the geomagnetic elements' value on the sample points and its mean value of the whole track. It can be expressed as follows:

$$\begin{cases} \overline{f} = \frac{\sum\limits_{k=1}^{n} f(k)}{n} \\ \delta = \sqrt{\sum\limits_{k=1}^{n} \left(f(k) - \overline{f}\right)^2} \end{cases} \tag{15}$$

where $\overline{f}$ is the average value of the geomagnetic vector corresponding to each sample path in the search area, and δ is the corresponding standard deviation.

The geomagnetic gradient S represents the anisotropic rate of change in the geomagnetic value on the sample track. It can be expressed as follows:

$$\begin{cases} S_l(\lambda, \varphi) = [f(\lambda+1, \varphi+1) + f(\lambda, \varphi+1) + f(\lambda-1, \varphi+1) \\ \qquad - f(\lambda+1, \varphi-1) - f(\lambda, \varphi-1) - f(\lambda-1, \varphi-1)]/6 \\ S(\lambda, \varphi) = \sqrt{S_x(\lambda, \varphi)^2 + S_y(\lambda, \varphi)^2} \end{cases} \tag{16}$$

where $S_l(\lambda, \varphi)$ is the geomagnetic change rate at a point in the x or y direction of the two-dimensional geomagnetic map, and $S(\lambda, \varphi)$ is the gradient of each geomagnetic element on the model class.

The correlation coefficient ρ represents the smoothness and volatility of the region where the sample path is located through the degree of correlation between data. It can be expressed as follows:

$$\begin{cases} \rho_x = \sqrt{\frac{1}{a(b-1)} \sum\limits_{\lambda=1}^{a} \sum\limits_{\varphi=1}^{b-1} \left(f(\lambda, \varphi) - \overline{f}\right)\left(f(\lambda, \varphi+1) - \overline{f}\right)} \\ \rho_y = \sqrt{\frac{1}{(a-1)b} \sum\limits_{i=1}^{a-1} \sum\limits_{j=1}^{b} \left(f(\lambda, \varphi) - \overline{f}\right)\left(f(\lambda+1, \varphi) - \overline{f}\right)} \\ \rho = \frac{\rho_x + \rho_y}{2} \end{cases} \tag{17}$$

where ρ_x and ρ_y are the roughness of each magnetic vector along the sample path in the x and y directions.

Geomagnetic information entropy H represents the degree of geomagnetic data confusion in the region where each sample track is located. It can be expressed as follows:

$$\begin{cases} H = -\sum\limits_{\lambda=1}^{a} \sum\limits_{\varphi=1}^{b} P(\lambda, \varphi) \log P(\lambda, \varphi) \\ P(\lambda, \varphi) = \frac{|f(\lambda, \varphi)|}{\sum\limits_{\lambda=1}^{a} \sum\limits_{\varphi=1}^{b} |f(\lambda, \varphi)|} \end{cases} \tag{18}$$

3.4. Two-Stage NN Training and Navigation

3.4.1. Training Sample Set Generation

The difference between the non-fully connected neural network in the second stage and PNN in the first stage lies in its negative feedback learning link, which requires a comparison of the loss function with the 'label' based on the forward calculation results, followed by a reduction in the loss function below the threshold, which is a sample learning training process.

Referring to the PNN pattern class construction method, in the process of making training sample sets for non-fully connected neural networks, grid the navigation area with the INS track and error range to generate a pattern class with the same number of grid points. The steps for creating a sample path dataset are as follows:

1. Generate a 20×20 magnetic map using multiple magnetic dipoles simulation;
2. Grid the magnetic map area with a resolution of 50 m;
3. Use the center point of the magnetic map as the endpoint, and generate a reference path with an error of (1600 m, 1600 m) and a corresponding true path. In order to generate training sets and test sets, the path sampling points are 20, and the length is set to 6 km (half training samples, half test samples);
4. According to the rules of the pattern recognition principle in Figure 1, 10,201 pattern classes (10,201 sample tracks) are created within a range of 5 km horizontally and vertically from the center point. Translate the real track 50 m in the positive and negative directions to generate two additional sample tracks that are considered to be accurate tracks (label tracks). Adding the real track, a total of 10,204 training sample sets were obtained. Mark the one real track and label tracks in the region as label '1', and label the remaining pattern tracks as "0". The generation of training sample sets is realized. The principle of sample production is shown in Figure 9.

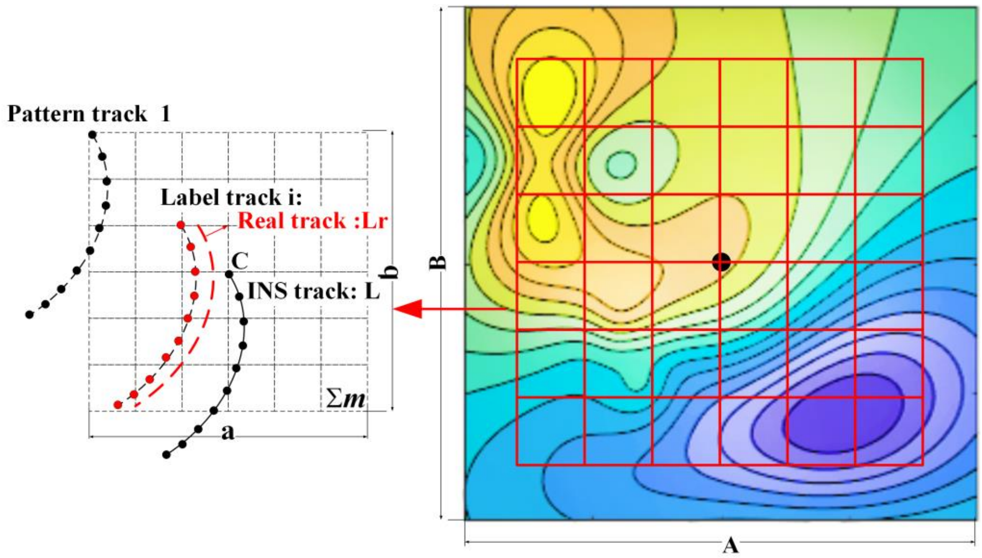

Figure 9. Sample set production principle.

On the right side of Figure 9, A and B are the boundary dimensions of the large-scale magnetic map, which are 20 km; on the left, a and b are matching regions that generate pattern tracks based on the error range, with a boundary size of 5 km and a resolution of 50 m. The pattern track numbers are $i = (1, 2, \cdots, m)$, and m is the total number of sample path datasets, 10,204 in total.

3.4.2. Geomagnetic Navigation Steps Based on Two-Stage Neural Network

The geomagnetic vector navigation algorithm based on two-stage NN can be summarized into the following steps:

1. Build the non-fully connected model by following the feature extraction and training steps in Sections 3.3 and 3.4;
2. Cascade the PNN and non-fully connected NN;

3. Follow these steps to prepare the input at the second stage of the non-fully connected NN:
    ① In the first stage of PNN, the input is still the same geomagnetic vector measurement sequence, and the output of PNN is changed into more pattern classes, which have a probability of 98%;
    ② According to Equations (15)–(18), calculate the geomagnetic vector features of the output tracks in the first stage.
4. The input features are sent into the trained non-fully connected NN in step 1. The best track is filtered and selected from all pattern classes.

4. Model Training and Simulation

Firstly, according to the sample set generation step, a magnetic dipole model is utilized to generate a regional magnetic map with a size of 20×20 km^2, and the magnetic map is gridded into a matching region with a resolution of 50 m. The magnetic map generated by simulation is shown in Figure 10.

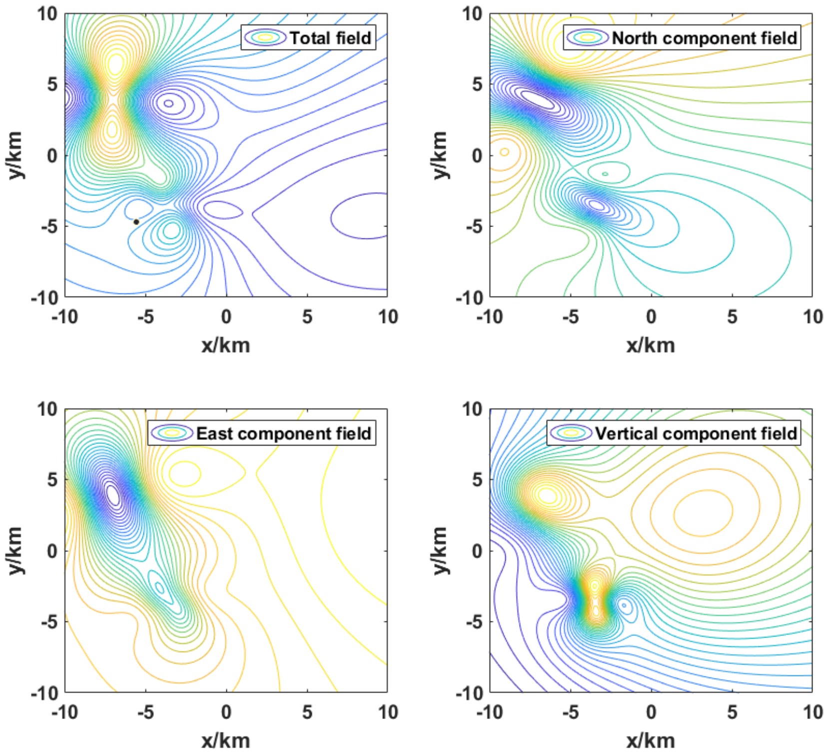

Figure 10. Simulated geomagnetic field map.

Next, generate a training dataset according to the previous training sample generation steps and label each path according to the definition of the label in the training sample set. Take the first 10 points of each path as training data and the last 10 points as test data.

Then, according to Equations (15)–(18), the vector and scalar features of each training datum in the matching region are extracted, and the two-stage neural network model is trained and tested with a test dataset. Table 5 shows the results of sample classification judgment using the two-stage neural network.

Table 5. Two-stage neural network binary classification judgment results.

Estimated Value / True Value	1	0
1	3	0
0	20	10,184

The evaluation indicators are calculated according to Equation (14), and the results are shown in Table 6.

Table 6. Calculation results of evaluation indicators for two-stage neural network.

Evaluating Indicator	0
Accurate rate	99.80%
Detection rate	100%
False alarm rate	0.19%

As can be seen in Table 6, the classification method based on the two-stage neural network has a high classification accuracy in geomagnetic two-component matching, reaching 99,8%, and the false alarm rate is only 0.19%.

The effectiveness of the algorithm is verified on this basis. The PNN-based neural network pattern recognition and the trained two-stage neural network model are used to perform path matching localization for 15 consecutive segments, respectively. The simulation parameter settings are the same as in Table 1. The results of 1000 Monte Carlo simulations are shown in Table 7, and the comparison results of PNN mismatches are shown in Figure 11.

Table 7. Comparison of navigation results of pattern recognition PNN and two-stage NN.

Method	Average Error/m	Success Rate
Pattern recognition PNN	87.48	92.45%
Two-Stage NN	70.71	98.13%

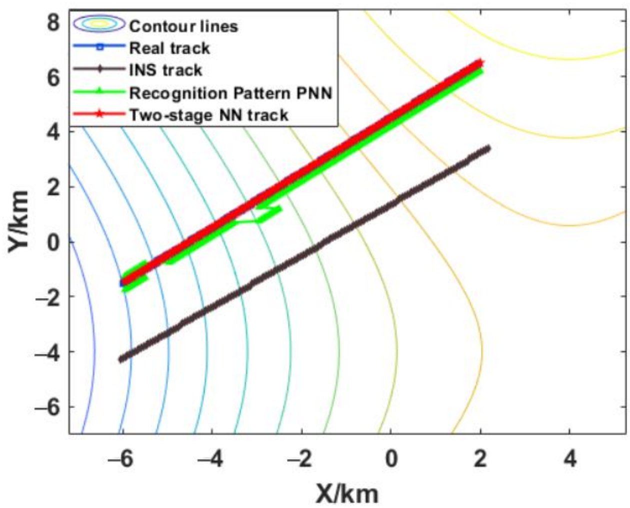

Figure 11. Comparison of pattern recognition PNN and two-stage NN tracks.

According to the comparison results in Figure 11 and Table 7, the two-stage neural-network-based geomagnetic vector navigation algorithm further improves the matching success rate and stability on the basis of pattern recognition based on PNN. Through a combination of coarse and precise screening, it achieves a positioning success rate of 98.13% and an average positioning error of 70.71 m in small-gradient regions of the geomagnetic field, proving that the proposed method has better robustness.

5. Experiment and Discussion

After the simulation experiment, the proposed method is tested by utilizing the actual flight experiment.

5.1. Experiment Preparation

The experimental data are obtained by airborne measurement on the Cessna-208 aircraft. The geomagnetic strapdown measurement system is mounted on the fiberglass package at the tail of the aircraft, which is an extension rod, as shown in Figure 12.

Figure 12. Experimental aircraft with strapdown navigation system.

Interpolation construction of the geomagnetic vector geomagnetic map is conducted using survey lines. Based on the Kriging interpolation method, the aeromagnetic survey data on the survey lines are interpolated and gridded, with a grid resolution of 100 m, and corresponding scalar and vector geomagnetic field maps are drawn, as shown in Figure 13. The average gradient of the geomagnetic field in the experimental region is shown in Table 8.

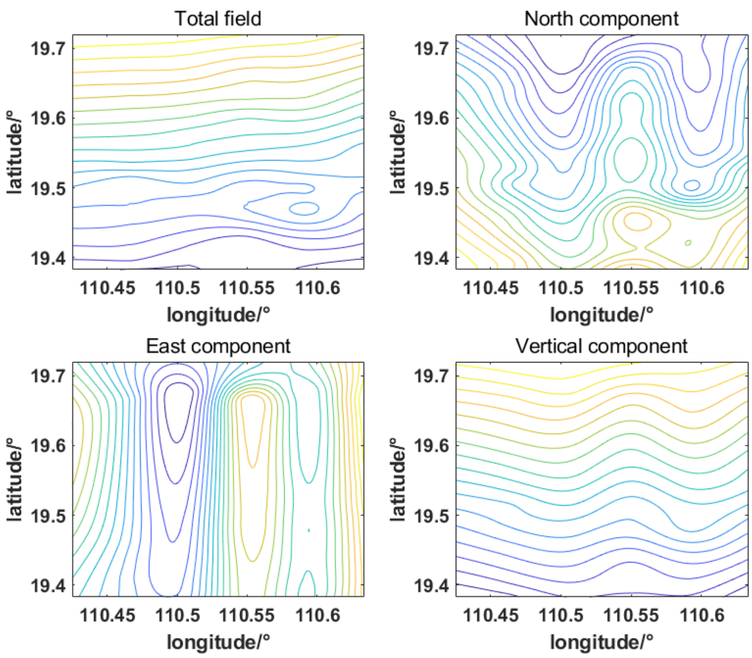

Figure 13. Geomagnetic field in the experiment region.

Table 8. Average geomagnetic gradient in the experimental region.

Geomagnetic Components	Average Gradient Value/nT·km^{-1}
total component	6.49
north component	3.16
east component	7.17
vertical component	19.37

5.2. Results and Discussion

According to Table 8, the average gradient of the geomagnetic vector in the experimental region is slightly greater than 11 nT/km, where the gradient is small and the region is a barren region with geomagnetic characteristics. The VICCP, VMAGCOM, recognition PNN, and two-stage NN navigation method are tested and compared based on the flight survey data of the experiment. The position results are shown in Figure 14 and Table 9.

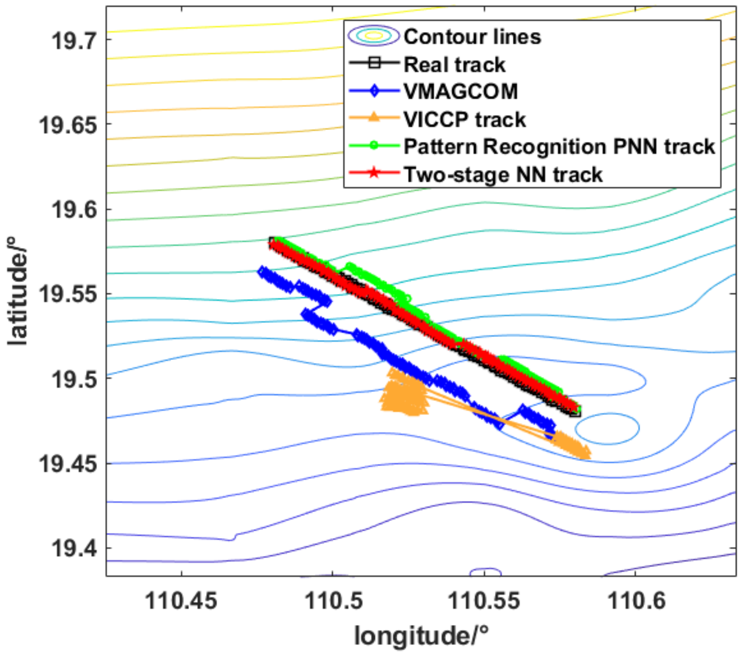

Figure 14. Comparison of four geomagnetic navigation methods based on flight survey data.

Table 9. Comparison of navigation results of four geomagnetic navigation methods.

Method	VICCP	VMAGCOM	Pattern Recognition PNN	Two-Stage NN
Average error/m	6636.14	2235.21	148.76	39.01
Maximum error/m	7061.26	2943.82	533.04	179.78
Standard deviation/m	2591.11	163.07	230.75	45.83
Success rate	0	0	75.10%	99.42%

As shown in Figure 14 and Table 9, in the real geomagnetic background field of the experimental region, due to the poor geomagnetic characteristics of the gradient, the traditional VICCP and VMAGCOM algorithm completely failed, and the positioning results are divergent. The pattern recognition navigation algorithm based on PNN has an average positioning error of 148.76 m and a 75.10% success rate, meaning that it has limited navigation capabilities for poor geomagnetic vector information. However, the geomagnetic vector navigation method based on a two-stage neural network presents bravo positioning error and success rate, which are, respectively, 39.01 m and 99.42%. It proves that outputs in the first stage of PNN were successfully and accurately screened in the second stage of the two-stage neural network.

6. Conclusions

To overcome the failure problem of traditional geomagnetic navigation algorithms based on correlation matching in geomagnetic barren areas, a new geomagnetic vector navigation method based on a two-stage neural network was proposed. In the first stage, a PNN model was established. Based on Bayesian optimal decision making, probability calculations were performed on the pattern classes in the navigation area, and the pattern classes of probability value at 98% were provided for the next stage as the first-stage outputs. By cascading PNN and non-fully connected networks, the input information composed of geomagnetic vector components and their characteristic parameters were sent to the second stage, a non-fully connected network, for precise screening, finally achieving high-precision neural network navigation. The VICCP, VMAGCOM, pattern recognition algorithm based on PNN and two-stage neural network-based geomagnetic vector navigation method was tested and compared by utilizing flight survey data. Thus, the proposed method was proved to have the best positioning error (39.01 m) and highest success rate (99%) in the experiment, which means that the proposed method has optimal robustness and adaptability for geomagnetic vector navigation in small-gradient geomagnetic field.

Regarding the real application of geomagnetic vector navigation on an airborne platform, larger areas with larger databases must be considered. However, since PNN is a feedforward neural network, it is 2–5 orders of magnitude faster in computational speed than neural networks, such as BP, RBF, CNN, etc. In the first stage of PNN in the proposed two-stage network, the calculating speed is fast enough to finish the real-time navigation mission. Additionally, in the second stage of the non-fully connected NN, with prior knowledge of the geomagnetic field maps, it could filter the optimal results from the PNN outputs, thereby achieving the judgment and screening of the optimal path. Thus, the proposed method has strong progressiveness and development potential and is worth further research and application.

Author Contributions: Conceptualization, Z.C. and Z.L.; methodology, Z.C.; software, Z.C.; validation, M.P.; formal analysis, Z.L.; investigation, D.C.; resources, Y.X.; data curation, Z.C and Y.X.; writing—original draft preparation, Z.C.; writing—review and editing, Z.L and Q.Z.; visualization, Z.C and Y.X.; supervision, Q.Z.; project administration, M.P.; funding acquisition, M.P. All authors have read and agreed to the published version of the manuscript.

Funding: This research was funded by the Natural Science Foundation of Hunan Province under Project 2021JJ40687.

Data Availability Statement: The data supporting this study's findings are available from the corresponding author upon reasonable request.

Conflicts of Interest: The authors declare no conflict of interest.

References

1. Canciani, A.; Raquet, J. Absolute Positioning Using the Earth's Magnetic Anomaly Field. *Navig. J. Inst. Navig.* **2016**, *63*, 111–126. [CrossRef]
2. Goldenberg, F. Geomagnetic navigation beyond the magnetic compass. In Proceedings of the Position, Location, And Navigation Symposium (Proceedings of IEEE/ION PLANS), San Diego, CA, USA, 25–27 April 2006.
3. The United States Department of Defense. Strategy for the Department of Defense Positioning, Navigation, and Timing (PNT) Enterprise. Available online: https://rntfnd.org/wp-content/uploads/DoD-PNT-Strategy.pdf (accessed on 12 March 2023).
4. Wang, W.; Meng, F. Multi-source Autonomous Navigation System Technology under National Comprehensive PNT System. *Navig. Control.* **2022**, *21*, 1–10.
5. Ge, Y.; Xue, L. Analysis of the Development Trends of US Army PNT Capability. *Navig. Position. Timing* **2019**, *6*, 12–18.
6. Chen, Z.; Liu, Z. An Improved Geomagnetic Navigation Method Based on Two-Component Gradient Weighting. *IEEE Geosci. Remote Sens. Lett.* **2022**, *19*, 1–5. [CrossRef]

7. Karshakov, E.; Tkhorenko, M. Aeromagnetic Gradiometry and Its Application to Navigation. *Autom. Remote Control* **2018**, *79*, 897–910. [CrossRef]
8. Wu, F. Study on Geomagnetic Vector Matching Navigation Technology. Master's Thesis, National University of Defense and Technology, Changsha, China, 2017.
9. Wang, Z.; Zhang, Q. A New Potential-Field Downward Continuation Iteration Method Based on Adaptive Filtering. *IEEE Trans. Geosci. Remote Sens.* **2022**, *60*, 1–11. [CrossRef]
10. Xu, C.; Yang, S. A new method for continuation of 3D potential fields to a horizontal plane. *Geophysics* **2003**, *68*, 1917–1921. [CrossRef]
11. Chen, Z.; Zhang, Q. A New Geomagnetic Matching Navigation Method Based on Multidimensional Vector Elements of Earth's Magnetic Field. *IEEE Geosci. Remote Sens. Lett.* **2018**, *15*, 1289–1293. [CrossRef]
12. Liu, W.; Wu, Z.; Wu, M.; Wu, Z. Geomagnetic matching technology based on Iterative Contour Matching algorithm. In Proceedings of the IEEE 2011 10th International Conference on Electronic Measurement and Instruments (ICEMI), Chengdu, China, 20–23 June 2011.
13. Li, M.; Liu, Y.; Xiao, L. Performance of the ICCP algorithm for underwater navigation. In Proceedings of the 2014 International Conference on Mechatronics and Control (ICMC), Jinzhou, China, 3–5 July 2014.
14. Xiao, J.; Duan, X. An improved ICCP matching algorithm for use in an interference environment during geomagnetic navigation. *J. Navig.* **2020**, *73*, 56–74. [CrossRef]
15. Xu, N.; Wang, L. An innovative PSO-ICCP matching algorithm for geomagnetic navigation. *Measurement* **2022**, *193*, 110958. [CrossRef]
16. Chen, K.; Liang, W. Multi-geomagnetic-component assisted localization algorithm for hypersonic vehicles. *J. Zhejiang Univ.-Sci. A* **2021**, *22*, 357–368. [CrossRef]
17. Pang, Y.; Zhou, Z. An INS/geomagnetic integrated navigation method for coarse estimation of positioning error and search area adaption applied to high-speed aircraft. *IEEE Sens. J.* **2023**, *23*, 7766–7775. [CrossRef]
18. Xie, S.; Li, B. MAGCOM and simulation of basic matching algorithm. *Aerosp. Control* **2008**, *26*, 55–68.
19. Chen, L.; Wang, S. An Improved Magnetic Field Contour Matching Algorithm Based on Ant Colony Optimization. *Electron. Opt. Control* **2010**, *17*, 8.
20. Liu, W.; Zhang, J. Multidimensional Fingerprints Method for Indoor Mobile Trajectory Mapping with Geomagnetic Information. *J. Electron. Inf. Technol.* **2013**, *35*, 2397–2402. [CrossRef]
21. Liu, Y.; Wu, M.; Hu, X. Contour constraint based geomagnetic matching method. *Chin. J. Space Sci.* **2007**, *27*, 505–511. [CrossRef]
22. Wu, F.; Zhang, Q.; Pan, M. Study on geomagnetic vector matching algorithm based on ICCP. *China Meas. Test* **2018**, *44*, 103–107.
23. Stateczny, A. Artificial neural networks for comparative navigation. In Proceedings of the Artificial Intelligence and Soft Computing-ICAISC 2004, Zakopane, Poland, 7–11 June 2004.
24. Algabri, M.; Mathkour, H.; Ramdane, H.; Alsulaiman, M. Comparative study of soft computing techniques for mobile robot navigation in an unknown environment. *Comput. Hum. Behav.* **2015**, *50*, 42–56. [CrossRef]
25. Stateczny, A.; Błaszczak-Bak, W.; Sobieraj-Złobińska, A.; Motyl, W.; Wisniewska, M. Methodology for processing of 3D multibeam sonar big data for comparative navigation. *Remote Sens.* **2019**, *11*, 2245. [CrossRef]
26. Kim, D.; Bang, H. Approach to geomagnetic matching for navigation based on a convolutional neural network and normalised cross-correlation. *IET Radar Sonar Navig.* **2019**, *13*, 1323–1332. [CrossRef]
27. Wang, Q.; Zhou, J. Triangle matching method for the sparse environment of geomagnetic information. *Optik* **2019**, *181*, 651–658. [CrossRef]
28. Zhou, J.; Liu, Y.X. Geomagnetic matching algorithm based on the probabilistic neural network. *Proc. Inst. Mech. Eng. Part G J. Aerosp. Eng.* **2011**, *225*, 120–126. [CrossRef]
29. Specht, D. Probabilistic Neural Networks. *Neural Netw.* **1990**, *3*, 109–118. [CrossRef]
30. Wang, P.; Hu, X. Matching suitability analysis for geomagnetic aided navigation based on an intelligent classification method. *Proc. Inst. Mech. Eng. Part G J. Aerosp. Eng.* **2014**, *228*, 271–283. [CrossRef]
31. Wang, L.; Yu, L.; Qiao, N. Analysis and simulation of geomagnetic map suitability based on vague set. *J. Navig.* **2016**, *69*, 1114–1124. [CrossRef]